Journal of Propulsion and Power
Vol. 24, No. 3, May–June 2008

Low-Heat-Load-Vane Profile Optimization, Part 1: Code Validation and Airfoil Redesign

Jamie J. Johnson* and Paul I. King†
Air Force Institute of Technology, Wright–Patterson Air Force Base, Ohio 45433
and
John P. Clark‡
U.S. Air Force Research Laboratory, Wright–Patterson Air Force Base, Ohio 45433

DOI: 10.2514/1.28530

Historically, there has been a distinct difference between the design of turbomachinery airfoils for aerodynamic performance and that for durability. However, future aeroengine systems will require ever-increasing levels of turbine inlet temperature, causing the durability and reliability of components to be an ever-more-important design concern. As a result, the need to incorporate heat-transfer predictions into traditional aerodynamic design and optimization systems presents itself. The following is an effort to design a minimized-heat-load airfoil with reputable aerodynamics. A Reynolds-averaged Navier–Stokes flow solver is validated over different flow regimes and various boundary conditions against extensive data available in literature. A nominal vane airfoil midspan profile is redesigned for minimum heat load by means of both design practice and two types of optimization algorithms. Results indicate an appreciable reduction in theoretical heat load relative to the original vane; peak leading-edge heat transfer was reduced and suction-surface transition onset was delayed significantly. A method for two-dimensional design optimization for aerodynamics and heat load is successfully demonstrated.

Nomenclature

b_x = axial chord
M = Mach number
P = pressure
Re = Reynolds number
s/s_t = fractional surface distance
T = temperature
Tu = freestream turbulence level
u_τ = wall friction velocity
x = axial direction
y = tangential direction
$y+$ = near-wall grid-thickness Reynolds number
Δy = near-wall grid element height
ν = kinematic viscosity

Subscripts

in = inlet condition
0 = total flow property
2 = exit condition

I. Introduction

GAS-TURBINE engine components are achieving increasingly better aerodynamic performance and high-pressure loading at design conditions. However, turbine durability issues are becoming the focus of more turbine design programs, because many component problems are ultimately traceable to those involving heat transfer. Therefore, a detailed understanding of the operating environment of turbine components should ideally precede a design for optimum aerodynamic performance. For example, it can be argued that developing a turbine that has traded off some aerodynamic qualities in favor of good thermal performance that yields a relatively long life is better than one with optimum aerodynamic qualities and a shortened operating life due to a poor thermal design. Turbine components are subject to significant thermal stresses and high temperatures and, as such, are constantly susceptible to failure mechanisms such as hot corrosion, high-temperature oxidation, and thermal fatigue. Measures including internal cooling passages, external film cooling, ceramic materials for structural members, and thermal barrier coatings have all been implemented by industry in an effort to combat the unfavorable effects of excessive surface heat transfer. Yet these technologies have been more often used on vanes and blades with geometries designed solely for aerodynamic performance. Because aircraft engines of the future demand ever-increasing performance levels, higher turbine inlet temperatures, and higher thrust-to-weight ratios, accurate turbine heat-transfer models are becoming more critical to gas-turbine design. This effort, reported in greater detail in [1], suggests including heat-transfer optimization of turbine airfoils in the traditional design for aeroperformance. That is, the work suggests a unification of traditionally separate disciplines of turbine durability and aerodynamics.

This investigation focuses on subduing aerodynamic characteristics commonly associated with increased heat transfer (including transition, freestream turbulence, and pressure gradients), all by means of manipulation of the airfoil 2-D profile geometry. The logical place to begin this effort is in the hottest part of the turbine, in which extremely high turbine inlet temperatures exist: the leading edge (LE) of the nozzle guide vane. The first step to ensuring that turbine components do not fail under their harsh operating

Presented as Paper 3386 at the 9th AIAA/ASME Joint Thermophysics and Heat Transfer Conference, San Francisco, 5–8 June 2006; received 24 October 2006; revision received 6 August 2007; accepted for publication 19 November 2007.

*Captain, U.S. Air Force; Student, Department of Aeronautics and Astronautics, 2950 Hobson Way. Member AIAA.

†Professor, Department of Aeronautics and Astronautics, 2950 Hobson Way. Senior Member AIAA.

‡Senior Analyst, Turbine Branch, Propulsion Directorate, 1950 Fifth Street. Member AIAA.

environment is the accurate prediction of the characteristics of heat transfer on the turbine vane, which can improve service life and reduce cooling requirements. The transport properties of laminar and turbulent flows are very different; therefore, proper prediction of overall heat transfer to turbine vanes and blades is critically dependent on the knowledge of the location and length of the transition between these two regimes. Understanding boundary-layer development is also essential to knowing the surface heat flux; controlling those aspects that contribute to excessive heat-transfer magnitude by way of profile shape design is one possible solution. As prediction methods have evolved, the forthcoming techniques will offer an innovative and modern approach to designing 2-D turbine vane airfoil geometries explicitly for reduced surface heat transfer.

Generally, heat transfer and early transition have not been major concerns on the pressure side (PS) of turbine inlet guide vanes, on which mostly favorable pressure gradients exist. Although the gas temperatures on the pressure (concave) side of an airfoil are high, rarely does the flow on a vane in cascade become fully turbulent, although the pressure-side boundary layers can see small areas of turbulence followed by a relaminarization (Nicholson et al. [2]). On the other hand, because transition to turbulence on the suction side is much more prevalent, due to the adverse pressure gradient experienced by the flow near the trailing edge (TE) of an airfoil, this will be an area of interest for this work.

The challenge is to create an airfoil geometry that keeps the boundary layer laminar and gradually accelerates the flow over the suction side, staving off transition to turbulence for as long as possible toward the trailing edge. The will be one main design goal. Though a tradeoff exists: as a laminar boundary layer is accelerated (i.e., $\mathrm{d}P/\mathrm{d}x \ll 0$), the boundary layer thins, causing higher surface temperature gradients and higher heat flux. Then again, the layer has not become turbulent, which causes further mixing and increased skin friction. Finally, although a thicker boundary layer insulates better, a thick turbulent boundary layer causes higher heat transfer than with a comparable laminar layer. Achieving delayed transition reduces the amount of surface over which turbulence occurs, thus decreasing overall surface heat transfer. The second overall vane design goal relates to lowering the leading edge at the heat transfer at the inlet at which the magnitude is highest.

To perform these designs efficiently, accuracy is necessary to design the airfoils, and by validating existing computational codes, this can be achieved. A nominal airfoil with extensive known experimental data concerning its heat transfer and pressure loadings was selected for code validation, and a new airfoil will be designed for reduced heat transfer. Ideally, this will yield increased confidence in numerical heat-transfer prediction and optimization methods for reduced heat load.

Historically, the design of turbine components specifically for reduced heat transfer has been rather limited, perhaps due to the complexities of accurately modeling heat transfer in realistic turbine environments, which often contain 3-D, unsteady, secondary, transonic, and turbulent flows. Little has been done concerning direct optimization of airfoils specifically for reduced heat transfer, with the exception of Nicholson et al. [2]. Their work used vanes with PS optimized geometries and found that suction-side (SS) transition was very common and moved forward with increasing Reynolds number Re and that increased inlet turbulence intensity Tu causes augmented mean heat-transfer rates. Similar trends were seen in the predictions of the current work. The study was effectively built on the prospect of minimizing heat transfer via boundary-layer control methods and it was concluded that aerodynamic efficiency is not compromised by a heat-transfer-optimized design. However, a number of researchers have used computational fluid dynamics (CFD) in conjunction with optimization techniques in other areas of study. Clark et al. [3] used 3-D time-resolved CFD to predict unsteady forcing levels on a single-stage high-pressure turbine blade to ultimately explore asymmetric vane spacing designs and use gradient-search optimization techniques to redesign the suction side of a blade. First-torsion stresses in this work were successfully reduced by 50%, resulting in a prototype engine that reduced resonant stresses by 36%. Optimization algorithms have also been used extensively since the mid-1990s to solve a wide range of optimization problems using objective functions. More specifically, genetic algorithms (GAs) have been successfully employed in the past by Durbin et al. [4], Obayashi and Tsukhara [5], and Anguita et al. [6] to define optimally contoured infinite cascade endwalls, maximize the lift coefficient of a wing airfoil, and design a turbine blade with low loss and high loading, respectively. These and many other works since then advocate the preferred use of genetic algorithms for design-space exploration, and these will be used in the redesign and optimization of the nominal turbine vane in the current work.

II. Code Validation and Airfoil Optimization Methodology

A. CFD Code Validation

To begin this effort, it was necessary to both validate a code for aerothermal predictions and to select a baseline airfoil for the design. The code used in this effort is a quasi-three-dimensional viscous fluid dynamics analysis tool for axial flow turbomachinery vane and blade rows named Wildcat by Dorney and Sondak [7]. This study will be restricted primarily to 2-D, because it only deals with an airfoil geometry at midspan. The Wildcat code has the ability to predict steady or unsteady flowfields for single or multiple blade rows and to generate grids for the calculations using another code called WILDGRD. For simplicity, the code in general will be referred to as Wildcat. The analysis is performed mathematically using the numerical solution of the Navier–Stokes equations. The numerical technique used in the solution is a time-marching, implicit, upwind finite difference scheme with a zonal, mixed-grid topology. It is second-order accurate in time and third-order accurate in space. The details of this Navier–Stokes numerical scheme can be reviewed in Dorney and Davis [7]. The code solves the flowfield on two overset grids, O and H, which are used to make the sequential temporal numerical calculations through the vane passage.

Next, an airfoil with an extensive pressure-loading and heat-transfer database at a wide range of conditions was selected for validation. This baseline airfoil, which will be referred to from here on as the nominal (nom) vane, is a highly loaded transonic turbine nozzle guide vane that experienced extensive aerothermal cascade testing by Arts et al. [8] using a short-duration isentropic light-piston compression-tube facility. The measurements were taken to examine several combinations of freestream flow parameters, primarily Reynolds number, Tu, and Mach number M, to ultimately assess aerodynamic performance and convective heat-transfer characteristics. The nom vane was a logical choice, because the original intent of this experimental database was to use the data for validation of both inviscid and viscous calculation methods. The original test program consisted of seven blade-velocity-distribution (pressure-loading) runs and 21 convective heat-transfer runs with varied freestream conditions according to the following ranges: $T_0 = 420$ K, $M_2 = 0.7$ to 1.1, $Re_2 = 5 \times 10^5$ to 2×10^6, and $Tu =$ 1.0 to 6.0%. Figure 1 shows the nom vane geometry plotted on fractional axial chord coordinates with the position of the flow-passage throat indicated.

The computational grid employed a near-wall grid-thickness Reynolds number of $y+ = (\Delta y u_\tau)/\nu \leq 1.0$ all around the airfoil surface. Commonly, $y+ < 1$ is acceptable for the k-ω model, in which the solution field is integrated to the wall, and $y+ < 3.0$ is acceptable for the Baldwin–Lomax turbulence model [9] used in this case by the Wildcat code. The size in I–J coordinates of the O grid is $I = 121$ by $J = 23$, whereas the size of the H grid is $I = 60$ by $J = 30$. The O grid has a near-wall grid element height $\Delta y = 1.27$ μm.

The Wildcat code was embedded in an easy-to-use turbine design and analysis system (TDAAS) used by many turbine component designers. The design system employed commercially available software and allowed the user to have a graphical user interface (GUI) for efficient operation of the grid generator and flow solver code. Using the Wildcat code in the design system, once an airfoil coordinate geometry was entered into the code, a grid of the desired

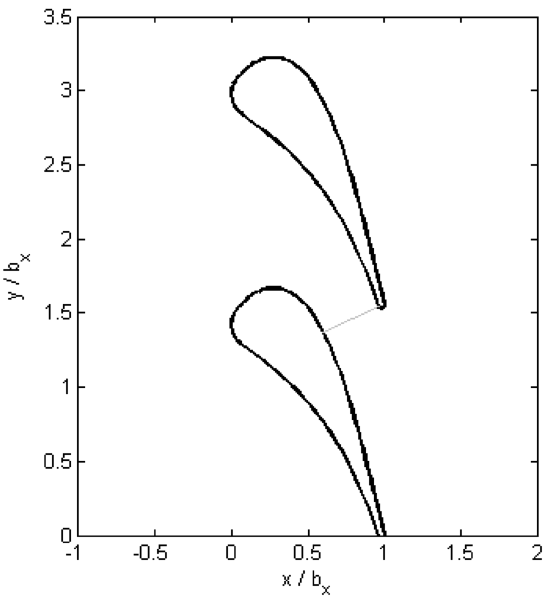

Fig. 1 Cross-sectional shape of the nom vane.

type was generated, all the necessary flow condition parameters and desired number of iterations were entered, and the code was executed. The code ultimately computed the resulting flowfield properties as they apply to heat transfer, pressures, Mach numbers, and boundary-layer characteristics. The Wildcat code was used to input the appropriate unique flow conditions for each run and simulate all seven of the pressure-loading and all 21 of the convective-heat-transfer trials performed experimentally [8] and to compare the code output with the data produced by the nom vane. Pressure-loading and heat-transfer predictions were run to convergence (between 10,000 and 40,000 iterations). This was shown to be adequate by convergence plots of each run. Key variable boundary conditions that were entered before each run included the following: the steady-state isentropic exit Mach number, total temperature upstream of the vane, total pressure upstream of the vane, freestream turbulence level, and vane wall boundary condition. Because the data in [8] provided the wall temperature for each of the heat-transfer runs, only the Dirichlet condition was used for validation purposes. Turbulent flow was modeled with the Reynolds-averaged Navier–Stokes equations with a turbulence model. Wildcat assumed transition onset as defined by a number of models. For validation purposes only, the Abu-Ghannam and Shaw (AGS) [10] transition model was chosen to be studied against the original data from Arts et al. [8]. These Wildcat runs were repeated until a wide enough set of flow conditions was covered to deem the code validation complete for the experimental data of the nom vane and the relative Wildcat results.

B. Airfoil Redesign and Optimization

Optimization of the nom vane for reduced heat transfer was a rigorous, iterative design and computation process. The design and analysis system for turbine airfoils was critical to the optimization task. The basic methodology as it applies to the current study is as follows. The system employs an industry-standard airfoil-shape-generation algorithm developed to define turbine blade and vane shapes. The grid generator and flow solver of Dorney and Davis [7] are used to determine the aerothermodynamic behavior of the design shapes. The shape and grid generators and the flow solver are then combined with GUI-based flowfield-interrogation and design-optimization techniques to allow a designer to realize new and/or improved airfoils quickly. The optimization can proceed via either gradient-based sequential quadratic programming (SQP) or genetic algorithms, and a wide range of objective functions are specifiable by the user. For example, it can be used to reduce loss, manipulate the pressure-loading characteristics of an airfoil, or minimize heat flux at specified areas for an airfoil surface, as is the focus of this study. Among other advantages, this design system allows reverse engineering in which the user can specify the desired flow characteristics or performance goals and generate a new airfoil shape based on these.

At first, the main idea of this work was to reduce the overall heat load on the optimized vane relative to the nom vane. This objective may be ambiguous, because the optimized airfoil may have a lower integrated heat load over both the pressure and suction surfaces than that with the nom vane, but may have one or more hot spots that would cause failure of surface material integrity in an actual engine test. Ideally, the new airfoil must also perform well aerodynamically (low loss and high loading) and have reduced surface heat-transfer characteristics when tested either computationally or experimentally. Also, the redesign and optimization process is a balance of both good engineering judgment and extensive parameter analysis. The two main objectives of the optimization were to 1) reduce LE heat transfer and 2) drive back transition on the SS as far possible toward the TE.

Knowing that heat flux is heat transfer per unit area, if the area is increased, heat flux must decrease to obtain the same heat load. Thus, the larger the radius of curvature, the lower the level of heat flux [11]. To achieve the goal of reduced LE heat transfer, the leading-edge-diameter (LED) parameter of the airfoil was increased. Extensive attention was given to this objective in hand iterations (changing parameters by hand and rerunning Wildcat repeatedly), and the overall vane properties were checked periodically for suitability. The design-log history showing all plots ensured that designs were becoming more favorable and guaranteed an efficient design progression. The current best airfoil was accepted and run in Wildcat with slight changes in parameters and immediately compared with previous designs. Concerning the second objective, optimization of the airfoils was conducted using an inverse design method in which the deviation between the design loading and a target pressure loading was minimized. This method allowed recent pressure-loading output plots to be manipulated by the user, in which the ensuing run would attempt to achieve a design nearest the changes made while staying within prescribed design limits. SQP algorithms were the type of optimization used here. It is a generalization of Newton's method for unconstrained optimization in that it finds a step away from the current point by minimizing a quadratic model of the problem. It replaces the objective function with a quadratic approximation and replaces constraint functions with linear approximations.

During the redesign of the nom vane it was determined (from the AGS transition model [10] that derived the start of transition from the turbulence level and pressure-gradient parameter and from design practice with the interactive GUI) that driving the minimum SS $P/P_{t,\mathrm{in}}$ back toward the TE of the airfoil generally resulted in delayed transition. This assumes that the minimum SS $P/P_{t,\mathrm{in}}$ was arrived at with as little oscillation in pressure gradient as possible. The airfoil pressure-loading results from a Wildcat run could be examined, and the inverse design method, as mentioned before, was used to successively find a design with a minimum SS total inlet pressure-ratio point closer to the TE. This approach successfully arrived at the delayed theoretical transition characteristics of the final optimized vane selected.

Physically, flow turning (75 deg) was kept constant between the nom and redesigned vane. The height-to-axial-length-ratio range was limited to 0 to 2.5. Fairly wide ranges were assigned to the leading- and trailing-edge radii, and the Bézier curves for the pressure- and suction-side shapes, which comprised the majority of the 16 airfoil profile parameters that were varied in the study design space. Slider bars for each of these variables within the turbine design system allowed realization of real-time changes in the shape of the airfoil, which helped with the quick resolution of design candidates from which to begin either of the optimization techniques used in this work. This close monitoring of curvature, area, and thickness distributions with axial chord and refined design-practice knowledge occurred before any aerothermal performance was assessed and compared with the nom vane.

Another tool used in the airfoil optimization process was a genetic algorithm. GAs have been used frequently in recent aerodynamic design practice for optimization purposes [5,6]. They can readily locate an optimal point in a problem space of theoretically infinite dimensions. In other words, much like the SQP algorithm, the turbine designer can vary several parameters and input desired ranges of these parameters related to the quantity optimized. Genetic algorithms are a process for function optimization that mimic the reproductive process experienced by biological organisms. The GA uses fitness functions prescribed by the user to determine the best option available. Fitness functions were used that best represented the priority of the airfoil parameters that were being optimized, such as heat transfer, which was a result of multiple other parameters. Careful implementation of a fitness function, which is subjective to the designer, will result in a significantly improved airfoil in an acceptable time by using the process of natural selection to improve the set of parameters, or genes, that describe the airfoil. Here, the nature of the fitness functions stayed close to the two main goals of optimizing to reduce LE heat load and manipulating the SS curves to delay transition toward the vane TE. A population size of 40 was chosen and the number of generations for this case was 38. The initial code structure, variables used, and methodology that laid the groundwork for commanding the desired objectives in the fitness functions relating to reduced heat-transfer design were previously developed within the lab. The approximate average computation time for the genetic algorithm operations alone to find a heat-transfer-optimized airfoil was approximately five days. Figure 2 is a flowchart with the elementary steps of the design sequence for the optimization genetic algorithm. Constraints of the optimization of the nom vane included keeping the axial chord constant (at 2.178 cm) for simplicity and interchangeability when it came time to test each vane cascade using a shock tunnel and a single set of flow conditions ([8] MUR237 cascade heat-transfer experimental run) in future work.

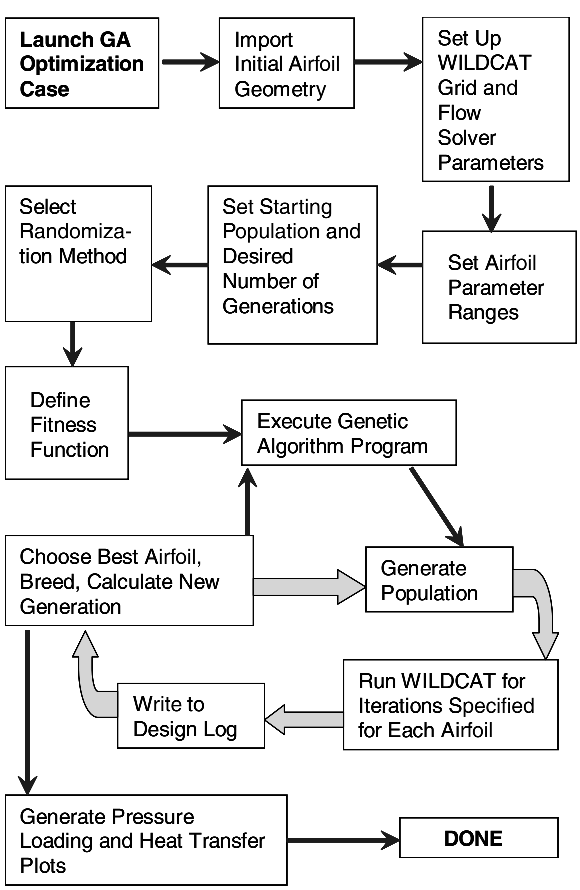

Fig. 2 Genetic algorithm process methodology.

These flow conditions were chosen for their applicability to a realistic modern turbine inlet environment and because they would match the conditions for turbulence grid-installed shock-tunnel tests to be done later to determine experimental heat transfer for both vanes.

In summary, the nom vane originally tested by Arts et al. [8] was redesigned to the desired lowered-heat-transfer specifications using the following steps:

1) The airfoil was run through numerous automated SQP optimization iterations to reduce overall heat load.

2) Knowing that the objective of step 1 was too ambiguous and unsatisfied with the results in that step, the two main objectives stated before were enforced.

3) Inverse design methods embedded in commercially available software with SQP optimization were used to attempt to delay transition.

4) Hand iterations and good design judgment were used to aid in reducing LE heat load by examining airfoils with large LEDs that supplied a favorable starting position for the GA process.

5) The best airfoil obtained from the preceding process was entered into a 40 object by 38 generation GA that further explored the problem space, reiterating the objectives, and the best GA airfoil calculated was selected.

As a result, suitable airfoil geometry had been created that met the two main objectives pertaining to reduced surface heat load. Hereafter, the new geometry will be referred to as the low-heat-load (LHL) vane. Once a solution was found, the two airfoils could then be compared in the proper experimental forum.

III. Results and Discussion

A. Code-Validation Results

Historically, older 2-D heat-transfer prediction methods have commonly overpredicted heat-transfer rates on both surfaces of an airfoil, because the effect of transition to turbulence is not accounted for [12]. It is a common industry practice to use a fully turbulent prediction when designing turbine components and cooling systems, to be conservative with respect to durability. Thus, the attempt to ensure the Wildcat code gave realistic predictions when compared with data with varying aerodynamic parameters.

Because the pressure loading, or velocity distribution, results from Wildcat were relied on so heavily for the heat-load optimization of the nom vane, the 2-D pressure-loading cases for the original data were reviewed. A total of seven experiments were run by Arts et al. [8] to analyze the nom vane at three discrete transonic isentropic exit Mach numbers M_2. Figures 3a–3c display the nom vane experimental results and the numerical prediction for pressure loading plotted against a fraction of the axial chord by the Wildcat code for $M_2 = 0.84, 0.875$, and 1.02, respectively (the numbers 1, 2, and 3 represent repeated runs by Arts et al. [8], conducted to achieve these flow conditions). Total inlet pressures for the three increasing Mach number runs were 1.42, 1.46, and 1.58 atm (20.8, 21.4, and 23.2 psia), respectively. Also shown to the right of the loadings are local isentropic Mach number plots, showing the acceleration of the flow around the airfoil. More simulations are necessary at different conditions to compare aerodynamic loss, because the data of Arts et al. did not record loss at the conditions plotted here. The results clearly show that the code predicts the pressure-loading profile very well over both the PS and SS of the nom vane for the range of transonic isentropic exit Mach numbers. The prediction even fairs well for the supersonic shock regions of the SS for the $M_2 = 1.02$ case. There is a small disparity between the data and the prediction on the SS for lower M_2 runs, possibly due to complexities of the SS boundary-layer change from a favorable to an adverse pressure gradient.

The collection of heat-transfer runs performed were narrowed down to five cases for the purpose of comparison of the original nom vane experimental results by Arts et al. [8] and the Wildcat Reynolds-averaged Navier–Stokes prediction. The cases selected span a range of three discrete values of exit Reynolds number Re_2 and turbulence intensity level Tu for an approximate $M_2 = 0.80$, which matches the

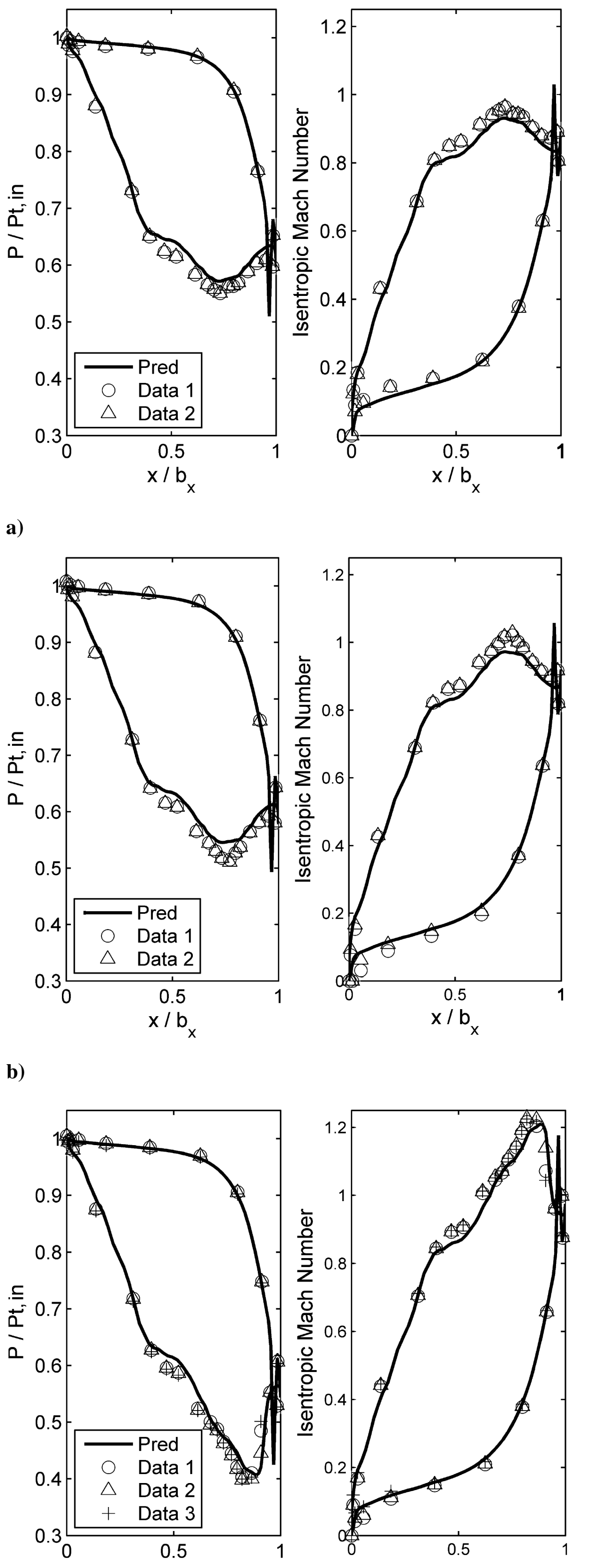

Fig. 3 Pressure-loading prediction for M_2: a) 0.84, b) 0.875, and c) 1.02.

values to be seen in the cascade shock-tube experimental comparison of the nom and LHL vanes. Table 1 gives the original names of the five runs and their respective key parameters, including total temperature and total pressure. The Reynolds number values are essentially 5×10^5, 10^6, and 2×10^6, whereas Tu is 1, 4, and 6%. The exact parameter values shown, except for Reynolds number, were entered into the TDAAS code as flow solver setup parameters to

Table 1 Selected Arts et al. [8] data for heat-transfer run flow conditions for code validation

Test name	M_2	Re_2	Tu, %	T_0, K	P_0, psia
MUR228	0.932	595,500	1.0	403.30	13.27
MUR247	0.922	2,117,000	1.0	416.20	49.24
MUR237	0.775	1,011,000	6.0	417.30	25.43
MUR218	0.760	1,007,000	4.0	413.50	25.29
MUR129	0.840	1,135,000	0.8	409.20	26.82

simulate each of these runs with the nom vane geometry. Figures 4a–4e show heat-flux distributions on the fractional surface distance (PS from -1 to 0 and SS from 0 to 1 on the x axis) of the nom vane for the Arts et al. [8] data, the Wildcat laminar viscous prediction, turbulent viscous prediction, the AGS [10] transition model prediction, and a triggered start of transition to compare with the data transition-onset locations for the five runs (shown in order in Table 1). By entering the fractional surface distance value for which the slope of the line first becomes positive in the data on the SS of the nom vane, Wildcat could perform predictions using the Arts et al. experimental transition-onset point (which is termed *hard trip* in the plots). The hard-trip function caused the laminar viscous equations to be evaluated up until the specified point of transition. In this way, a direct comparison of the suction-side transition could be observed between data and prediction; it could also be shown that by delaying transition, the overall heat load of the vane will decrease, because the integral heat flux for the hard trip is obviously less than for AGS [10]. It can be seen that both transition predictions are somewhat sudden. This is because AGS [10] is only a transition-start model in Wildcat and not a transition-length model, as can be seen in the disparity between the hard-trip AGS line and the Arts et al. [8] data. In addition, the AGS [10] model was derived from experiments performed solely on a flat plate, not on a turbine vane.

Many trends can be seen in the predictions. The predicted vane peak heat load at the leading edge and at the beginning of suction-side turbulence onset has a strong and relatively proportional Re_2 dependence. Suction-side transition is obviously prevalent even at lower Reynolds number runs, and so the heat-flux predictions provide good motivation for attempting to delay transition to reduce airfoil heat load in the optimization effort. All figures also present a heavy transition-onset-location dependence on Tu. As Tu increases, transition tends to occur earlier on the SS, which agrees with the work of Blair [13]. This trend was also observed for increasing Re_2. For constant $Tu = 1\%$ as Re_2 grew from 5×10^5 to 2×10^6, AGS [10] and hard-trip transition-onset locations on the SS moved back toward the stagnation point dramatically and the LE peak heat flux nearly tripled. Concerning the natural AGS and turbulent viscous predictions, there appears to be transition to turbulence at about the -0.1 location for all five runs, which accounts for the overprediction of heat transfer on the PS. For the most part, SS laminar predictions are good. On the PS, however, for the high Reynolds number case, the laminar boundary-layer heat transfer is overpredicted. In contrast, for the high-Tu case, the PS laminar heat flux is underpredicted, which tends to be in accordance with past studies that have experienced freestream turbulence heat-transfer augmentation due to possible secondary, unsteady, or turbulence-driven flow effects [14,15]. In addition, the laminar viscous prediction only accounts for shear in the boundary layer and has no inherent way to account for unsteady heat and mass transport due to higher levels of Tu. Overall, it appears that for transition to typical turbine levels of Re_2, the Wildcat code prediction performs with moderate integrity, especially for SS characteristics. Nonetheless, this fares better than most prediction comparisons performed in the past [16–18]. For high Tu, PS laminar heat transfer is underpredicted. For high Re_2, PS laminar heat transfer is overpredicted; however, the SS heat flux is captured well. A reputable 2-D Navier–Stokes code was validated against a good range of accurately obtained turbine-representative data, suggesting that the Wildcat code may be used for different turbine component design and optimization tasks.

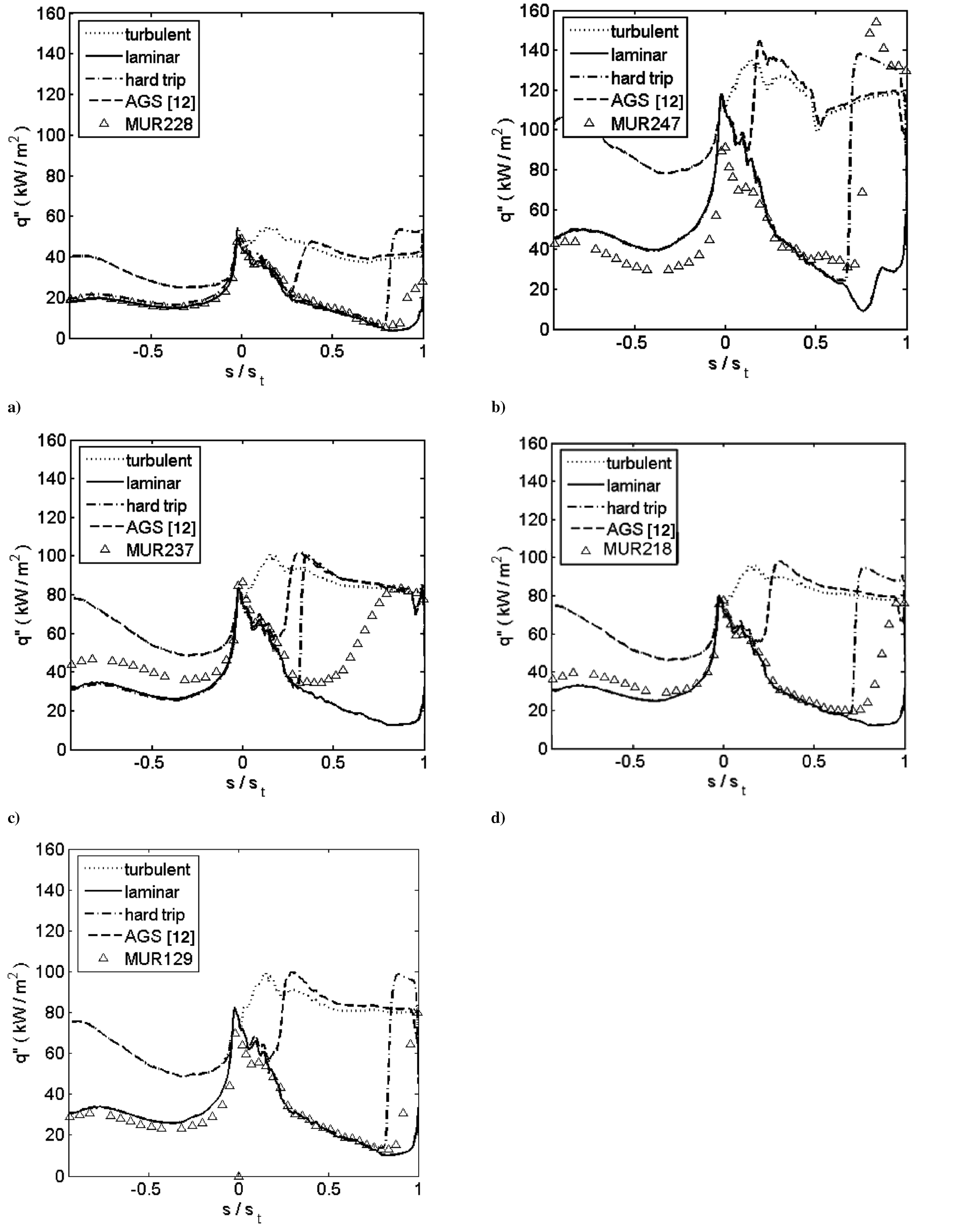

Fig. 4 Wildcat heat-flux surface distribution predictions for runs with a) low Reynolds number and low *Tu*, b) high Reynolds number and low *Tu*, c) medium Reynolds number and high *Tu*, d) medium Reynolds number and medium *Tu*, and e) medium Reynolds number and low *Tu*.

B. NOM Versus the LHL Airfoil

After the lengthy iterative process previously outlined was executed, the redesign and optimization of the nom vane for the objectives of reduced leading-edge heat transfer and delayed suction-side transition yielded favorable results. A direct comparison of the two vanes is given in this section to cover a wide range of aerothermodynamic flow characteristics and considerations.

The new LHL vane is different from the nom vane in that it has a slightly larger LED, resulting in a rounder, more even, LE structure that will serve to distribute the LE heat load. The LHL vane also has a

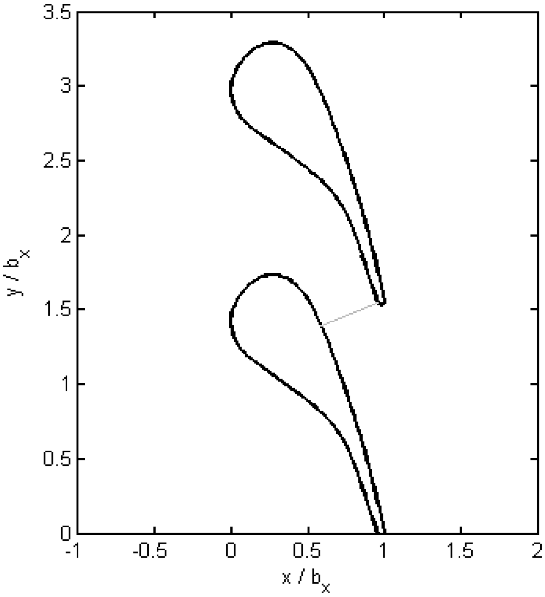

Fig. 5 LHL vane cross-sectional geometry.

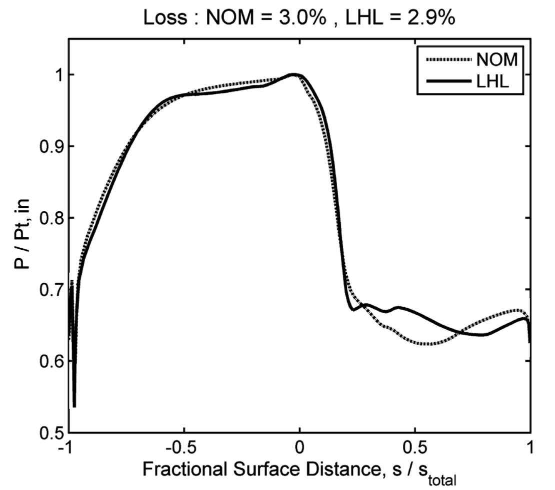

a)

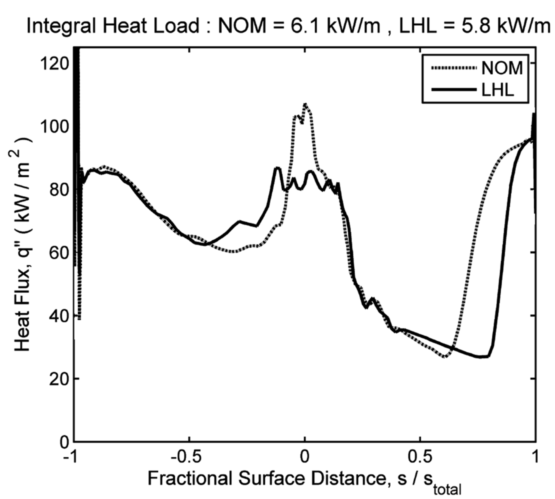

b)

Fig. 6 Prediction comparisons of the nom and LHL vanes using the AGS [10] transition model: a) pressure loading and b) heat-flux distribution.

thicker midchord and slimmer TE section for enhanced flow acceleration. Figure 5 is a first look at the reduced heat-transfer-optimized solution, showing the midspan cross-sectional airfoil geometry for the LHL vane.

To reiterate, the two main goals of the redesign process were to lower the LE peak heat load and delay the onset of transition on the SS as far as possible by driving the minimum static-to-total pressure ratio $P/P_{t,\mathrm{in}}$, or maximum Mach number, back as far as possible toward the TE. Many different airfoil shapes were observed during the process of the optimization. After many hours of computing time, the results were narrowed down to a healthy group of airfoil-geometry candidates. Table 2 compares the properties most relating to the goal of the reduced heat-transfer optimization for the original nom vane: the best airfoil that could be created by hand iterations and two good candidates that resulted from the GA. These candidates were gathered from the design-log history and stood out well above other designs. The coordinates x/b_x and $P_s/P_{t,\mathrm{in}}$ in the second column are for the point of the ratio of the minimum static to inlet total pressure on the suction side of the vanes. A higher value in x increased the probability of delayed transition, whereas a lower value in y showed a greater overall acceleration of SS flow in keeping the boundary layer laminar. The best GA airfoils given are the 987th and 1508th optimization iterations that resulted when the two objectives, which were translated into proper fitness functions, were enforced. The values were taken from Wildcat runs of the midspan geometries with the laminar viscous assumption.

Observing the values in Table 2, it is clear that the GA was very successful in realizing the two main optimization objectives. The 987 and 1508 airfoils gave impressive results, and so these two naturally stood out and were suitable as a final choice. From here, one airfoil had to be chosen to progress further in the study to be tested experimentally for reduced heat transfer. The aerodynamic losses, integral heat loads, and LE peak loads of the two GA airfoil solutions are essentially the same. Although the 987 airfoil has slightly better numbers for these three categories, it was eliminated in favor of the 1508 airfoil. Knowing that the two main objectives of the optimization, the peak loads were the same, and the fact that the 1508 airfoil moved the minimum pressure-ratio point toward the TE 5% of the surface distance over the 987 airfoil made the 1508 airfoil the appropriate choice. This is a significant design improvement for delaying transition with an x coordinate of minimum pressure ratio 24% closer to the TE of the wetted suction-surface distance than with the nom vane. Figures 6a and 6b compare the predicted pressure loadings and heat-flux surface distributions of the nom and LHL vanes by running the Wildcat code at the design conditions of MUR237 ($Re_2 = 10^6$, $M_2 = 0.8$, and $Tu = 4\%$) with the AGS [10] transition model. Because the flow over a turbine nozzle guide vane normally has laminar and turbulent regions with a transition between, on both the pressure and suction surfaces for most operating conditions, the focus of the heat-transfer comparison stayed with the AGS prediction. The laminar and turbulent prediction comparisons yielded similar trends. The nom curves are visually much smoother than those of the LHL, but the LHL vane would prove to be a much

Table 2 Final candidate airfoils from optimization process compared with the nom vane

Airfoil	Minimum SS $P/P_{t,\mathrm{in}}$ coordinate (x/b_x, $P/P_{t,\mathrm{in}}$)	Loss, %	Integral heat load, $\mathrm{kW/m^2}$	LE peak heat load, kW/m
NOM	(0.51, 0.61)	3.521	4.170	112.5
Best hand-iterated	(0.56, 0.63)	3.359	4.265	95.4
GA (987)	(0.70, 0.63)	3.118	4.248	96.0
GA (1508)	(0.75, 0.63)	3.198	4.271	96.1

better performing vane concerning all aspects of turbine vane performance. It can be seen that the LHL vane even has lower aerodynamic losses than the nom vane. Concerning separation, neither of the vane loading profiles indicate that this is an issue for this set of conditions. In addition, the pressure-side fluctuations of the LHL vane plot do not ultimately cause transition to turbulence, as seen in Fig. 6b.

The LHL vane clearly has a much lower leading-edge heat load, delayed transition by as much as 20% of the SS distance over the nom airfoil, lower integrated heat load, and better aerodynamic qualities with lower loss. Concerning downstream pressure perturbations that a blade may experience, the LHL vane also reduced the vane's exit-static pressure-ratio distortion by 3.3%. It is clear that the larger leading edge of the LHL vane worked well at evening out and lowering the peak heat load at the geometric stagnation point. Instead of spiking like the nom vane and creating a local hot spot, the heat flux stays low and fluctuates slightly, resulting in a 15% reduction in LE heat load. Although the PS heat flux is higher, the SS heat-transfer curve behaves well, indicating that the SS curvature is suitable. These factors all indicate that the computational optimization of the nom vane to the LHL vane with much better thermodynamic performance was a success. Both the main redesign and optimization objectives were realized and a worthy candidate was chosen that can be tested experimentally to verify that the same heat-transfer trends occur in a realistic environment. Finally, because the vane designs both perform the same duties regarding choking the combustor flow, providing transonic exit properties for the rotor inlet, and have the same flow turning, the relative performance of the two vanes should remain similar over a range of off-design throttle speeds (not the case for two different rotor blades). The SS (and, in consequence, the integral) heat load could be reduced by delaying transition as a result of moving the minimum SS pressure-ratio point back toward the TE as far as possible. Also, the leading-edge heat transfer was significantly reduced with the optimized vane design.

IV. Conclusions

A few favorable findings were made as a result of this study concerning both numerical prediction and reduced heat-transfer airfoil design optimization of turbine components. The Wildcat Reynolds-averaged Navier–Stokes flow solver was validated over a wide range of turbine inlet conditions (Re_2, M_2, and Tu), giving moderately accurate predictions of vane midspan heat transfer and very accurate pressure loading against an extensive database of light-piston compression-tube-facility experiments. The Wildcat code, in union with the TDAAS, was used with two types of optimization algorithms to generate an optimized turbine nozzle-guide-vane midspan geometry (LHL vane). The design successfully reduced leading-edge peak heat transfer by 15% and delayed suction-side transition 24% closer to the trailing edge than with the nom vane. In addition, for the AGS [10] transition model, the LHL vane showed lower midspan integral heat load and lower aerodynamic loss, suggesting that the optimized vane has more desirable aerodynamic qualities as well.

Acknowledgments

The authors would like to acknowledge the contributions of R. J. Anthony, M. Ooten, and J. Dagg for their technical support on this effort. Additional support from individuals from the U.S. Air Force Research Laboratory and the Air Force Institute of Technology are also greatly appreciated.

References

[1] Johnson J, J., "Optimization of a Low Heat Load Turbine Nozzle Guide Vane," M.S. Thesis, School of Engineering, Air Force Inst. of Technology, Wright–Patterson AFB, OH, Mar. 2006.

[2] Nicholson, J. H., Forest, A. E., Oldfield, M. L. G., and Schultz, D. L., "Heat Transfer Optimized Turbine Rotor Blades—An Experimental Study Using Transient Techniques," *Journal of Engineering for Gas Turbines and Power*, Vol. 106, Jan. 1984, pp. 173–182.

[3] Clark, J. P., Aggarwala, A. S., Velonis, M. A., Gacek, R. E., Magge, S. S., and Price, F. R., "Using CFD to Reduce Resonant Stress on a Single-Stage, High-Pressure Turbine Blade," IGTI ASME Turbo Expo, Amsterdam, The Netherlands, American Society of Mechanical Engineers Paper GT-2002-30320, 2002.

[4] Durbin, P., Eaton, J., Laskowski, G., and Vicharelli, A., "Transonic Cascade Measurements to Support Turbulence Modeling," *Contractors Meeting in Turbulence and Rotating Flows*, U.S. Air Force Office of Scientific Research, Arlington, VA, 2004, pp. 57–62.

[5] Obayashi, S., and Tsukhara, T., "Comparison of Optimization Algorithms for Aerodynamic Shape Design," *AIAA Journal*, Vol. 35, No. 8, Aug. 1997, pp. 1413–1415.

[6] Anguita, D., Cravero, C., Filz, C., and Rivieccio, F., "An Innovative Technique for the Aerodynamic Design of Turbine Blade Profiles Using Artificial Intelligence," 33rd AIAA Fluid Dynamics Conference, Orlando, FL, AIAA Paper 2003-3737 , 2003.

[7] Dorney, D. J., and Davis, R. L., "Navier–Stokes Analysis of Turbine Blade Heat Transfer and Performance," *Journal of Turbomachinery*, Vol. 114, Oct. 1992, pp. 795–806.

[8] Arts, T., Lambert de Rouvroit, L., and Rutherford, A. W., "Aero-Thermal Investigation of a Highly Loaded Transonic Linear Turbine Guide Vane Cascade," Technical Note 174, von Kármán Inst. for Fluid Dynamics, Rhode-Saint-Genèse, Belgium, Sept. 1990.

[9] Baldwin, B. S., and Lomax, H., "Thin Layer Approximation and Algebraic Model for Separated Turbulent Flows," AIAA Paper 78-257, 1978.

[10] Abu-Ghannam, B. J., and Shaw, R., "Natural Transition of Boundary Layers—The Effects of Turbulence Pressure Gradient and Flow History," *Journal of Mechanical Engineering Science*, Vol. 12, No. 5, 1980, pp. 1–18.

[11] Kays, W. M., and Crawford, M. E., *Convective Heat and Mass Transfer*, McGraw–Hill, New York, 1993.

[12] Dunn, M. G., "Convective Heat Transfer and Aerodynamics in Axial Flow Turbines," American Society of Mechanical Engineers Paper 2001-GT-0506, 2001.

[13] Blair, M. F., "Influence of Free-Stream Turbulence on Boundary Layer Transition in Favorable Pressure Gradients," *Journal of Engineering for Power*, Vol. 104, Oct. 1984, pp. 743–750.

[14] Galassi, L., King, P. I., and Elrod, W. C., "Effects on Inlet Turbulence Scale on Blade Surface Heat Transfer," AIAA Paper 90-2264, 1990.

[15] Clark, J. P., and Praisner, T. J., "Predicting Transition in Turbomachinery, Part 1: A Review and New Model Development," American Society of Mechanical Engineers Paper GT2004-54108, 2004.

[16] Wistanley, D. K., Booth, T. C., and Dunn, M. G., "The Predictability of Turbine Vane Convection Heat Transfer," AIAA Paper 81-1435, 1981.

[17] Dunn, M. G., Martin, H. L., and Stanek, M. J., "Heat-Flux and Pressure Measurements and Comparison with Prediction for a Low-Aspect-Ratio Turbine Stage," *Journal of Turbomachinery*, Vol. 108, July 1986, pp. 108–115.

[18] Rae, W. J., Taulbee, K. C., and Dunn, M. G., "Turbine-Stage Heat Transfer: Comparison of Short-Duration Measurements with State-of-the-Art Prediction," AIAA Paper 86-1465, 1986.

F. Liu
Associate Editor